DOI: 10.1002/ejic.201000802

Ruthenium Complexes Bearing N–H Acidic Pyrazole Ligands

Thomas Jozak,[a] Dirk Zabel,[a] Anett Schubert,[a] Yu Sun,[a] and Werner R. Thiel*[a]

Keywords: Ruthenium / Pyrazole / Hydrogenation / Ligand effects

Chelate ligands containing at least one pyrazole group were treated with $RuCl_2(PPh_3)_3$, $RuHCl(CO)(PPh_3)_3$ and $RuH_2(CO)(PPh_3)_3$ to form ruthenium complexes bearing protic N–H groups in close proximity to the catalytically active ruthenium centre. In the case of the hydridoruthenium complex $RuHCl(CO)(PPh_3)_3$ the resulting complexes also contain a basic hydrido ligand. The combination of acidic and basic hydrogen species in one molecule and the arising two-site reactivity was thoroughly investigated spectroscopically and by DFT calculations. Catalytic tests on the hydrogenation and transfer hydrogenation of acetophenone showed a general activity of these systems.

Introduction

Ruthenium(II) complexes play a dominant role in the catalytic (asymmetric) hydrogenation of carbonyl compounds. Depending on the ligands coordinated to the central metal and on the substrates, different mechanistic routes of hydrogen transfer are possible: (A) direct activation of dihydrogen, (B) transfer hydrogenation with alcohols (e.g. 2-propanol) as the hydrogen source or (C) metal–ligand-bifunctional hydrogenation. Whereas the substrate has to bind directly to the metal centre in (A) and (B),[1] the hydrogen transfer is performed differently in metal–ligand-bifunctional hydrogenation. Here, a parallel transfer of a hydrido ligand coordinated to the metal site and a proton derived from a protic group of one of the donor ligands occurs, which, in an ideal case, enhances the reaction rate significantly. Such protic groups can either be alcohols or amines or amine derivatives like sulfonamides, etc. Noyori et al. and others described a series of chiral ruthenium-based catalysts following these requirements and showing high activity and enantioselectivity in the hydrogenation of ketones and other substrates with polar C=E double bonds.[2]

In the present work ruthenium complexes of bi- (N,N-) or tridentate (N,N,N-) donors have been investigated, which include at least one pyrazole fragment with a protic NH group. Coordination of these ligands brings this NH group in close proximity to the metal site, and it becomes even more acidic due to the coordination of the Lewis-acidic metal site to the pyrazole moiety. We recently could show that such a coordination motif provides a proton donor site for the formation of strong hydrogen bonds.[3] This effect should also be beneficial for an improved catalyst–substrate interaction according to the metal–ligand-bifunctional hydrogenation pathway (Scheme 1).

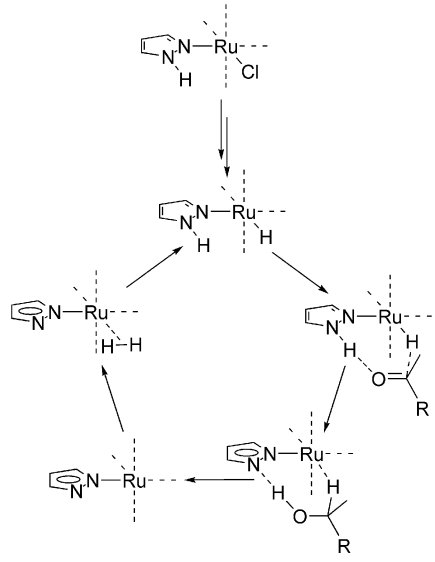

Scheme 1. Postulated reaction mechanism for the metal–ligand-bifunctional hydrogenation with pyrazole-based ligands.

Results and Discussion

Ligand Synthesis

During the last decade, a series of pyrazole-based ligands have been introduced for catalytic applications.[4] However, pyrazoles coordinated to ruthenium(II) catalysts have rarely been reported.[5] For investigations described in this article the pyrazole-derived ligands **1**–**3** (Scheme 2), all bearing NH groups at a pyrazole ring, were used to generate a series of novel ruthenium(II) complexes.

[a] Fachbereich Chemie, Technische Universität Kaiserslautern
Erwin-Schrödinger-Str. Geb. 54, 67663 Kaiserslautern, Germany
Fax: +49-631-2054676
E-mail: thiel@chemie.uni-kl.de

Supporting information for this article is available on the WWW under http://dx.doi.org/10.1002/ejic.201000802.

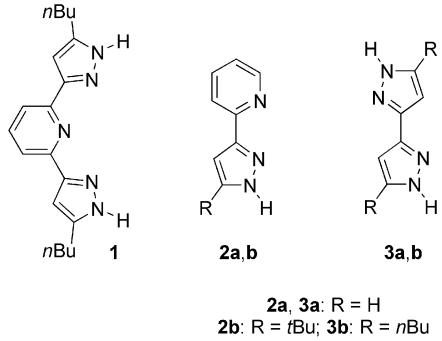

Scheme 2. Pyrazole ligands used for the synthesis of ruthenium(II) complexes.

The syntheses of the tridentate 2,6-bis(5-butylpyrazol-3-yl)pyridine (**1**), a structural analogue of the well-known 2,2′:6′6′′-terpyridine ligand, the bidentate 2-[3(5)-pyrazolyl]pyridines (**2a**, **2b**) and the bidentate 3,3′-bi(1*H*-pyrazole) (**3a**) were carried out according to published procedures.[6–8] Butyl side chains attached to the pyrazole ring were employed to enhance the solubility of the derived ruthenium complexes in organic solvents. The novel 3,3′-bi(1*H*-pyrazole) ligand **3b** was synthesized by performing a double Claisen condensation between diethyl oxalate and hexan-2-one in the presence of sodium methoxide (Scheme 3). The intermediate tetraketone was characterized solely by NMR spectroscopy. It undergoes keto/enol tautomerism where the enol form is the major isomer. The desired bipyrazole **3b** was obtained from the tetraketone by ring closure with hydrazine and purified by recrystallization from ethyl acetate.

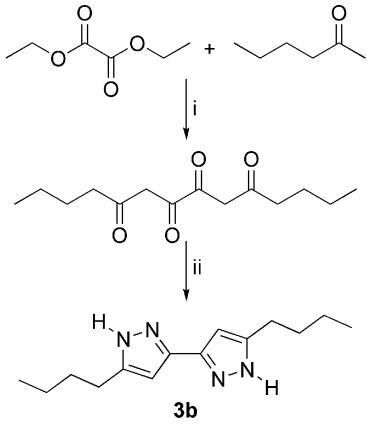

Scheme 3. (i) NaOMe, Et_2O, room temp., 45 h, 45%. (ii) N_2H_4, EtOH, 80 °C, 4.5 h, 42%.

The bipyrazole **3b** exhibits a sharp absorption for the N–H stretching vibration at 3400 cm^{-1} in the IR spectrum (KBr) that is typical for pyrazoles with N–H···N hydrogen bonds in the solid state.[9] Single crystals suitable for X-ray diffraction were grown by diffusion of pentane into a solution of **3b** in MeOH. The bipyrazole **3b** crystallizes in the tetragonal space group $I4_1/a$. Figure 1 shows the molecular structure of **3b**.

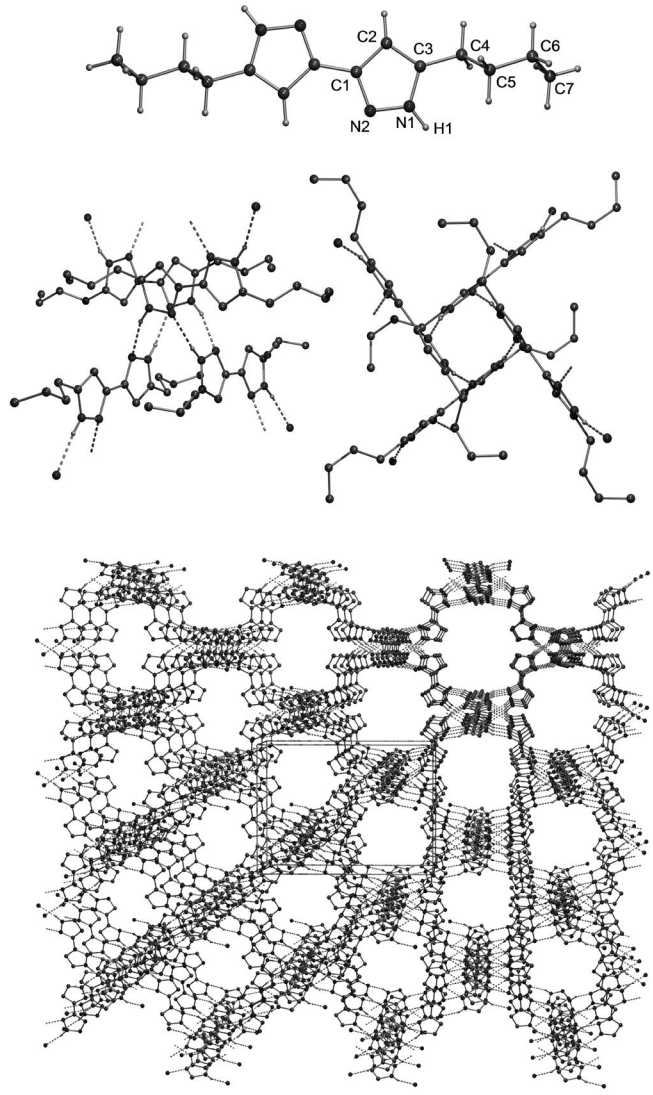

Figure 1. Top: molecular structure of **3b** in the solid state. Characteristic hydrogen-bond parameters: N1–H1 0.88 Å, H1···N2 2.02 Å, N1···N2 2.8728(17) Å; N1–H1···N2 163.00°. Centre: views of the linking pyrazole tetramers; the hydrogen atoms are omitted for clarity. Bottom: 3D-network structure (perpendicular to the *ac* plane) formed by the 3,3′-bi(1*H*-pyrazole) cores; the butyl side chains are omitted for clarity.

In its solid-state structure, **3b** includes a centre of symmetry at its central C–C bond (Figure 1, top). Both pyrazole rings act as proton-donating (N1) and -accepting (N2) sites for intermolecular hydrogen bonds. This results in the formation of a complex three-dimensional network structure, wherein pyrazole tetramers[3,9d,10] are involved as the linking centres (Figure 1, centre). The network contains three-dimensional pores, filled by the butyl chains.

Ruthenium Complexes

Three different ruthenium precursors, $RuCl_2(PPh_3)_3$ (**4**),[11] $RuHCl(CO)(PPh_3)_3$ (**5**)[12] and $RuH_2(CO)(PPh_3)_3$ (**6**),[12] were treated with the ligands **1**–**3**, which lead to different products as described below. Treatment of the

dichloridoruthenium complex $RuCl_2(PPh_3)_3$ (**4**) with the tridentate ligand **1** in dichloromethane yields the orange-coloured cationic species **7** with chloride as the counterion (Scheme 4).

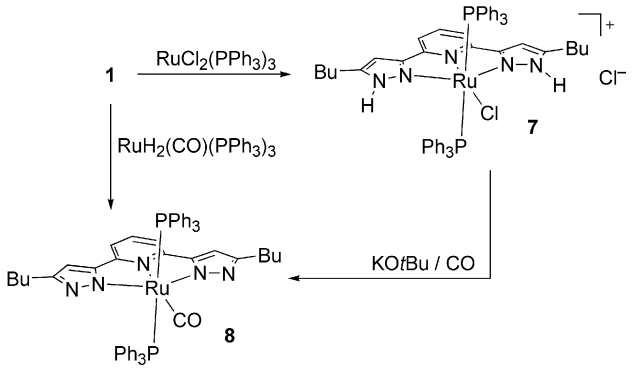

Scheme 4. Synthesis of the 2,6-bis(5-butylpyrazol-3-yl)pyridine complexes **7** and **8**.

The occurrence of the ligand N–H groups in **7** can clearly be seen by the N–H stretching absorption in the IR spectrum (3438 cm^{-1}). There is only one singlet at δ = 25.5 ppm in the $^{31}P\{^1H\}$ NMR spectrum and one resonance in the ^1H and $^{13}C\{^1H\}$ NMR spectra for each chemically different proton and carbon atom of the ligand. This proves, in combination with a single-crystal X-ray structure analysis, that the ruthenium centre has an octahedral coordination with a *trans* orientation of the phosphane ligands. Single crystals suitable for X-ray diffraction were grown by diffusion of pentane into a solution of **7** in MeOH. Compound **7** crystallizes in the monoclinic space group $P2_1/a$. Figure 2 shows the molecular structure of **7** in the solid state.

The structure of **7** is distinguished by the *trans* orientation of the phosphane ligands and by two different N–H···Cl hydrogen bonds. One of the N–H protons binds to the chlorido ligand coordinated to the ruthenium centre leading to a centrosymmetric dimer, the second N–H unit interacts with the chloride anion. There are several cationic ruthenium complexes with a similar set of ligands.[13] However, none of them provides protic N–H units for dimerization through hydrogen binding. The meridional coordination of the nitrogen donors seems to be favourable even if monodentate ligands like acetonitrile are used.[14] There are only a few examples of tridentate N,N,N-donors performing facial coordination as long as meridional coordination is sterically possible.[15] Additionally, only bidentate phosphanes are found to coordinate to ruthenium in a *cis* configuration.[10,16] The bond parameters around the ruthenium centre in compound **7** are in complete agreement with similar complexes in the literature. The Ru–N3 (pyridine) bond length is shorter than the other two Ru–N bond lengths due to the steric restrictions of the tridentate ligand and the weak chlorido ligand in the *trans* position to pyridine. Ru–N4 is about 6 pm longer than Ru–N2, probably due to the different hydrogen-bond motifs at the neighbouring nitrogen atoms.

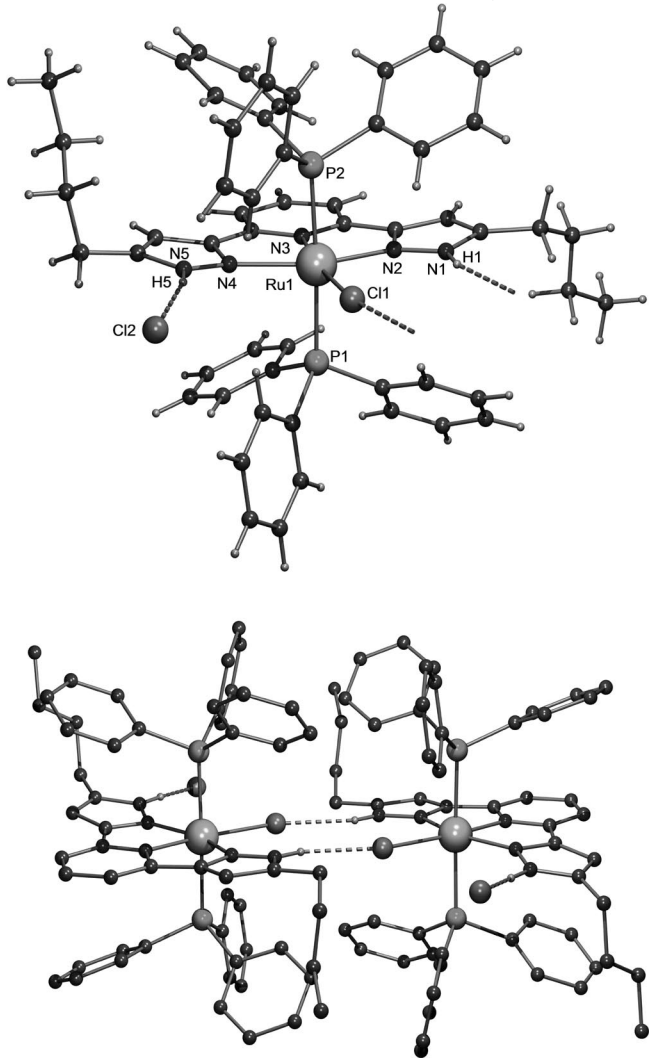

Figure 2. Top: molecular structure of **7** in the solid state; characteristic bond lengths [Å], angles [°] and torsion angles [°]: Ru1–Cl1 2.4605(8), Ru1–P1 2.3909(9), Ru1–P2 2.3897(10), Ru1–N2 2.056(3), Ru1–N3 1.983(3), Ru1–N4 2.118(3), N1–H1 0.88, H1···Cl1 2.41, N1···Cl1 3.242(3), N5–H5 0.88, H5···Cl2 2.25, N5···Cl2 3.104(4); Cl1–Ru1–P1 90.17(3), Cl1–Ru1–P2 89.69(3), Cl1–Ru1–N2 92.44(9), Cl1–Ru1–N3 170.56(9), Cl1–Ru1–N4 111.80(9), P1–Ru1–P2 176.62(4), P1–Ru1–N2 92.29(7), P1–Ru1–N3 90.09(8), P1–Ru1–N4 89.50(7), P2–Ru1–N2 91.09(7), P2–Ru1–N3 90.61(8), P2–Ru1–N4 87.42(7), N2–Ru1–N3 78.12(13), N2–Ru1–N4 155.70(12), N3–Ru1–N4 77.64(12), N1–H1···Cl1 159.00, N5–H5···Cl2 3.104(4); N3–C1–C6–N2 3.4(5), N3–C5–C9–N4–5.4(5). Bottom: dimeric structure of **7**.

To obtain models for metal–ligand-bifunctional hydrogenation catalysts bearing hydrido ligands at the ruthenium centre and protic N–H groups in close proximity, hydridoruthenium precursors were treated with the ligands **1**–**3**. If **1** is treated with the dihydrido complex **6**, the dipyrazolidoruthenium(II) complex **8** is formed in 15–20% spectroscopic yield (Scheme 4). It seems that in this case the basicity of the hydrido ligands is sufficient for a complete NH deprotonation of the N,N,N-chelate ligand. This is supported by an alternative access to **8**, which was opened up by bubbling CO through a solution of **7** in the presence of

KO*t*Bu (yield 59%). The IR spectrum of **8** is dominated by an intense band of the C=O stretching vibration at 1961 cm^{-1}. The signals for the N–H vibration observed in the IR spectrum of **7** have vanished. As compared to **7**, the ^{31}P resonance (δ = 32.0 ppm) is shifted by almost 6 ppm downfield. All ^{1}H NMR resonances of the N,N,N-chelate ligand are shifted upfield compared to those of **7**; whereas the ^{13}C NMR resonances remain almost unaffected.

Crystals suitable for X-ray diffraction were obtained by slow diffusion of pentane into a concentrated solution of **8** in toluene. The compound crystallizes in the monoclinic space group $P2_1/a$. Figure 3 shows the molecular structure of **8** in the solid state.

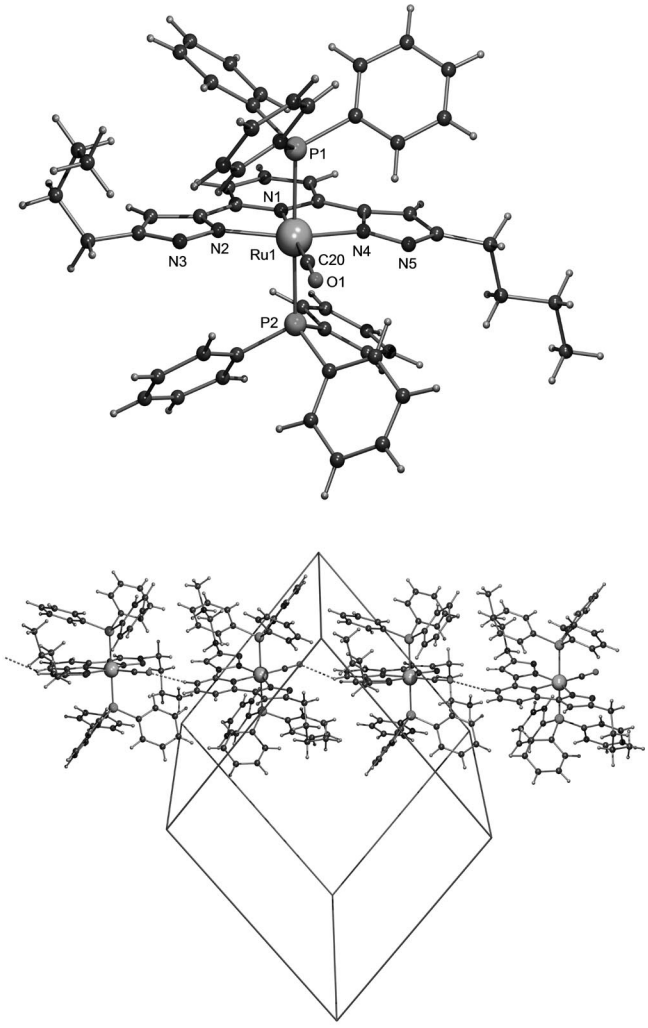

Figure 3. Molecular structure of **8** in the solid state; characteristic bond lengths [Å], angles [°] and torsion angles [°]: Ru1–P1 2.3828(17), Ru1–P2 2.3866(19), Ru1–N1 2.062(6), Ru1–N2 2.084(6), Ru1–N4 2.069(6), Ru1–C20 1.862(8), O1–C20 1.150(10); P1–Ru1–P2 178.14(7), P1–Ru1–N1 90.49(17), P1–Ru1–N2 86.72(17), P1–Ru1–N4 92.90(16), P1–Ru1–C20 89.3(3), P2–Ru1–N1 90.77(17), P2–Ru1–N2 94.91(17), P2–Ru1–N4 86.03(16), P2–Ru1–C20 89.5(3), N1–Ru1–N2 76.6(2), N1–Ru1–N4 77.8(2), N1–Ru1–C20 179.3(3), N2–Ru1–N4 154.4(2), N2–Ru1–C20 104.1(3), N4–Ru1–C20 101.5(3), Ru1–C20–O1 177.8(7); N1–C1–C6–N2 2.5(10), N1–C5–C9–N4 2.5(9).

There are just two examples of ruthenium(II) complexes where two phosphane centres, one carbonyl ligand and three nitrogen donors coordinate the metal site: $[TpRu(PPh_3)_2(CO)]^+$ and $[(dppe)Ru(CO)(MeCN)_3]^{2+}$.[17] Furthermore only a few structurally characterized ruthenium(II) complexes bearing anionic N-donors have been described up to now: three complexes with bridging imidazolido ligands,[18] one example wherein an aliphatic amido ligand is involved[19] and only two compounds where at least one deprotonated pyrazole coordinates to ruthenium(II).[20] This is quite astonishing, since similar amides have been postulated as intermediates in ruthenium-catalyzed hydrogenation reactions. The structural parameters of **7** and **8** can be compared directly: as expected, the Ru–P bond lengths are almost identical for both compounds. After the weak chlorido ligand in **7** is exchanged with the strong σ-donor CO group, the Ru–pyridine bond length becomes about 8 pm longer in **8**. The two Ru–pyrazole bond lengths are now almost identical. Despite the anionic nature of the pyrazoles in **8**, there is no significant change in the Ru–pyrazole bond lengths compared to those in **7**, probably because of the steric restrictions resulting from the tridentate ligand.

Treatment of **1** with the monohydrido complex **5** gives a complex mixture of products, which as yet have not been completely isolated and characterized. Addition of sodium perchlorate led to just a few crystals (yield < 5%) of a cationic carbonyl(hydrido)bis(triphenylphosphane)ruthenium(II) complex, wherein 2,6-bis(5-butylpyrazol-3-yl)pyridine acts as a bidentate donor (for structure see Supporting Information). One of the pyrazole units remains uncoordinated, both pyrazole N–H groups undergo hydrogen binding to the perchlorate anion. Here, the hydrido ligand of the starting material **5** seems to be unable to deprotonate the pyrazole.

We therefore extended our investigation to the bidentate ligands **2** and **3**, which gave, by treatment with the monohydrido complex **5**, the desired carbonyl(hydrido)bis(triphenylphosphane)ruthenium(II) complexes **9** and **10** in 65–85% yields (Scheme 5).

Complex **9a** was obtained in crystalline form by slow diffusion of *n*-pentane into a chloroform solution. It crystallizes with two crystallographically independent molecules and one molecule of chloroform per formula unit in the unit cell. Figure 4 shows the molecular structure of one of these molecules in the solid state. For the complete solid-state structure see the Supporting Information

Since pyridine is a stronger σ-donor than pyrazole, the hydrido ligand is found oriented in the *trans* position to the pyrazole unit (see below for spectroscopic discussion) and thus in an unfavourable position for a metal–ligand-bifunctional hydrogenation. The only way to overcome this problem is to change from pyrazolylpyridine to a bipyrazol ligand. Complex **10b** could be crystallized by slow diffusion of *n*-pentane into a solution of this compound in ethanol. The solvent is included in the crystalline material. Figure 5 shows the molecular structure of one of these molecules in the solid state.

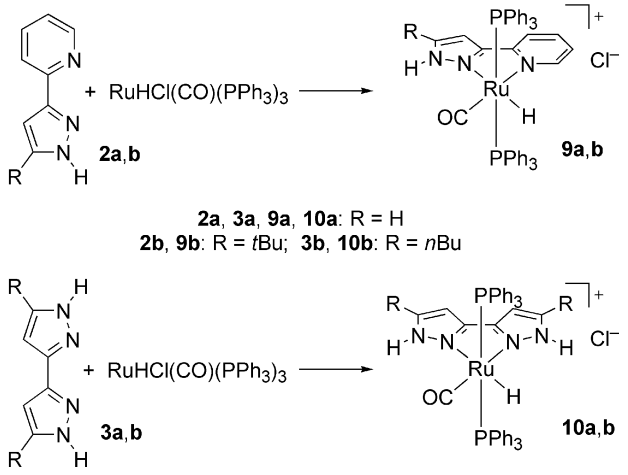

Scheme 5. Synthesis of the hydridocarbonylruthenium complexes **9** and **10**.

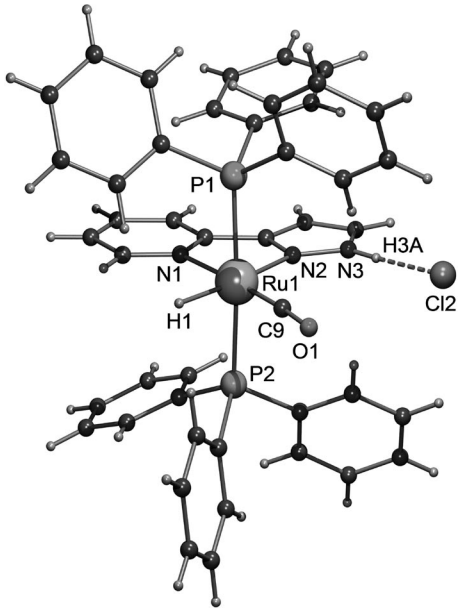

Figure 4. Molecular structure of **9a** in the solid state; characteristic bond lengths [Å], angles [°] and torsion angles [°]: Ru1–P1 2.3849(12), Ru1–P2 2.3453(12), Ru1–N1 2.159(3), Ru1–N2 2.180(3), Ru1–C9 1.835(4), Ru1–H1 1.77(3), N3–H3A 0.88, H3A···Cl2 2.19, N3···Cl2 3.066(3); P1–Ru1–P2 176.51(4), P1–Ru1–N1 87.43(8), P1–Ru1–N2 90.35(7), P1–Ru1–C9 93.00(12), P2–Ru1–N1 91.06(8), P2–Ru1–N2 92.29(7), P2–Ru1–C9 88.29(12), N1–Ru1–N2 74.78(11), N1–Ru1–C9 176.09(14), N2–Ru1–C9 109.10(14), P2–Ru1–H1 85.9(9), N1–Ru1–H1 94.7(10), P1–Ru1–H1 91.1(10), C9–Ru1–H1 81.4(10), N2–Ru1–H1 169.4(10), N3–H3A···Cl2 3.066(3); N1–C1–C6–N2 0.6(4).

In the solid state, the six-coordinate cationic ruthenium complexes **9a** and **10b** undergo hydrogen bonding to the chloride anion, leading to isolated ion pairs in the case of **9a**. Compound **10b** forms a one-dimensional hydrogen-bonded polymer structure, wherein both N–H units, the chloride anion and one additional molecule of ethanol are included. In **9a**, the Ru–N distances differ by about 2 pm due to a balance between the donor strengths of pyrazole versus pyridine and the donor strengths of the ligands in

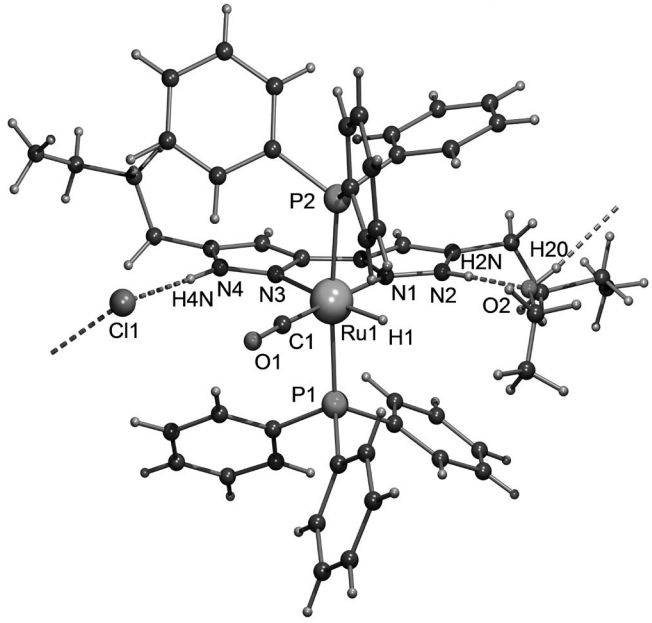

Figure 5. Molecular structure of **10b** in the solid state; characteristic bond lengths [Å], angles [°] and torsion angles [°]: Ru1–P1 2.3552(11), Ru1–P2 2.3542(10), Ru1–N1 2.119(3), Ru1–N3 2.183(3), Ru1–C1 1.813(4), Ru1–H1 1.60(4), N2–H2N 0.86(2), H2N···O2 1.86(2), N2···O2 2.710(6), O2–H2O 0.77(2), H2O···Cl1 2.25(2), O2···Cl1 3.013(3), N4–H4N 0.85(3), H4N···Cl1 2.25(3), N4···Cl1 3.082(3); P1–Ru1–P2 172.85(4), P1–Ru1–N1 90.19(9), P1–Ru1–N3 93.27(9), P1–Ru1–C1 88.87(13), P2–Ru1–N1 90.78(9), P2–Ru1–N3 93.80(9), P2–Ru1–C1 90.29(13), N1–Ru1–N3 73.60(11), N1–Ru1–C1 178.58(14), N3–Ru1–C1 105.41(15), C1–Ru1–H1 84.1(13), P1–Ru1–H1 85.8(13), P2–Ru1–H1 87.0(13), N1–Ru1–H1 96.9(13), N3–Ru1–H1 170.5(13), N2–H2N···O2 177(3), O2–H2O···Cl1 172(3), N4–H4N···Cl1 166(3); N1–C2–C5–N3 0.5(5).

the *trans* position (H^- and CO). This becomes clear when the Ru–N bond lengths of complex **10b** are discussed: here the strong σ-donating hydrido ligand leads to a pronounced increase of the Ru–N bond length in the *trans* position. Accordingly, the bond length between the ruthenium centre and the carbonyl carbon atom is slightly shorter in **10b**, reflecting the poorer σ-donor strength of pyrazole. The hydrido ligands in **9a** and **10b** could be located in the difference Fourier map. However, the Ru–H bond lengths differ largely [**9a**: 1.77(3) Å; **10b**: 1.60(4) Å], probably due to general problems with the exact location of the hydrido ligands in close proximity to the electron-rich metal sites, which is always subject to errors. In **10b** the hydrido ligand is located in the "correct" position to an N–H unit of one of the pyrazole moieties. The corresponding distance H1–H2N is 3.16(4) Å, which is rather ideal for the concerted Ru–H···C=O···H–N interaction with the carbonyl group of a substrate.

Complexes **9a**,**b** and **10a**,**b** were additionally characterized by elemental analysis, IR and NMR spectroscopy. The C=O stretching frequencies were found between 1952 and 1941 cm^{-1}; the Ru–H stretching vibrations could not be assigned. They are reported in the literature to appear at 1980–1950 cm^{-1},[12,17a,21] which is close to the intense C=O absorption, or to be unobservable because of their low in-

tensities.[22] The $^{31}P\{^1H\}$ NMR resonances of **9a**,**b** (δ = 46.3, 46.4 ppm) and **10a**,**b** (δ = 44.9, 43.9 ppm) are shifted by about 50 ppm downfield with respect to those of free triphenylphosphane. The ^1H NMR resonances of the hydrido ligands are found as triplets, shifted remarkably upfield (**9a**: δ = –12.50 ppm; **9b**: δ = –12.66 ppm; **10a**: δ = –12.19 ppm; **10b**: δ = –12.10 ppm) with coupling constants $^2J_{PH}$ = 19.8–20.4 Hz. In contrast, the resonances of the protic N–H units are shifted downfield (**9a**: δ = 16.41 ppm; **9b**: δ = 13.61 ppm; **10a**: δ = 12.82, 14.13 ppm; **10b**: δ = 12.26, 13.60 ppm). The differences between compounds **9** and **10** are not due to the different ligands but to the different solvents used for NMR spectroscopy. For compounds **10a** and **10b** two different N–H resonances are found since the two pyrazolyl units occupy chemically different coordination sites at the ruthenium centre.

Analogous reactions between the bidentate ligands **2a**,**b** and the dihydrido precursor $RuH_2(CO)(PPh_3)_3$ (**6**) give the corresponding neutral carbonylhydridopyrazolido complexes **11a**,**b** in high yields (Scheme 6). However, treatment of **3a**,**b** with $RuH_2(CO)(PPh_3)_3$ (**6**) did not result in the formation of the corresponding complexes **12** bearing a monodeprotonated bipyrazole ligand. The additional hydrido ligand should undergo reaction with the remaining N–H unit, similar to the formation of compound **8**. This will yield a pentacoordinate ruthenium(II) complex, which probably decomposes in solution.

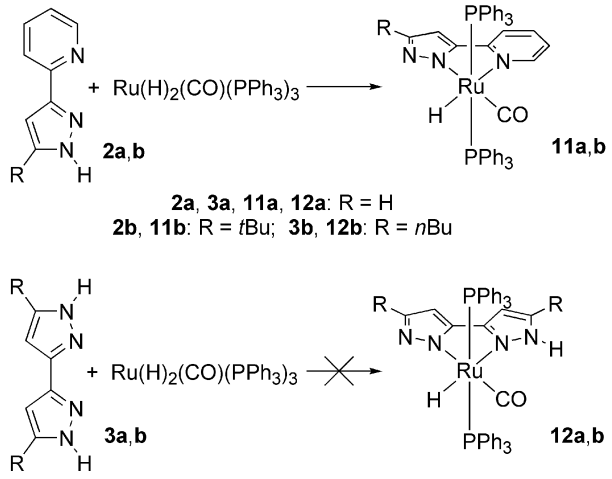

Scheme 6. Synthesis of the carbonylhydridoruthenium complexes **11**.

Theory

The metal–ligand-bifunctional hydrogenation of carbonyl compounds with such cationic ruthenium(II) complexes was calculated with a model system similar to compound **7**, wherein the chlorido ligand was replaced by a hydrido ligand, and the $P(C_6H_5)_3$ ligands were replaced by PMe_3. Formaldehyde was employed as the substrate. We used the DFT functional B3LYP[23] in combination with the 6-31G* basis set[24] for C, H, N, O, P and the LANL2DZ (ECP) basis set for Ru[25] (for details see Experimental Section and Supporting Information). The results are summarized in Figure 6 and Table 1.

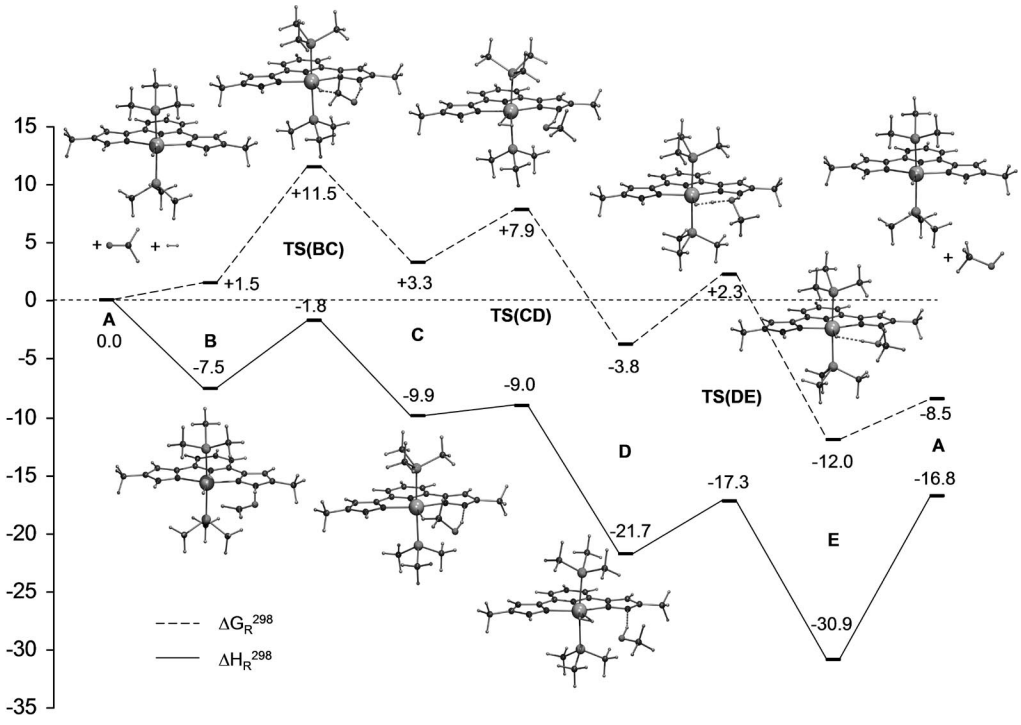

Figure 6. Results of the DFT calculation on the mechanism of the hydrogenation of formaldehyde catalyzed by a cationic ruthenium(II) complex with an N,N,N-donor ligand. ΔH_R and ΔG_R are given in kcal mol^{-1}.

Table 1. Results of the DFT calculations with B3LYP/6-31G*(LANL2DZ).

Compound	H_f, G_f [hartrees]	ΔH_f, ΔG_f [kcal mol^{-1}]	ΔH_f, ΔG_f [kJ mol^{-1}]
H_2	–1.162036		
	–1.176828		
CH_2O	–114.469832		
	–114.495307		
A	–1793.037347		
	–1793.133610		
A + H_2 + CH_2O	–1908.669215	0.0	0.0
	–1908.805745	0.0	0.0
B	–1907.519167		
	–1907.626542		
B + H_2	–1908.681203	–7.5	–31.8
	–1908.803370	+1.5	+6.2
TS(BC)	–1907.510028		
	–1907.610546		
TS1 + H_2	–1908.672064	–1.8	–7.5
	–1908.787374	+11.5	+48.2
C	–1907.522995		
	–1907.623711		
C + H_2	–1908.685031	–9.9	–41.5
	–1908.800539	+3.3	+3.7
TS(CD)	–1908.683531	–9.0	–37.6
	–1908.793190	+7.9	+33.0
D	–1908.703865	–21.7	–91.0
	–1908.811741	–3.8	–15.7
TS(DE)	–1908.696767	–17.3	–72.3
	–1908.802115	+2.3	+9.5
E	–1908.718532	–30.9	–129.5
	–1908.824868	–12.0	–50.2
CH_3OH	–115.658700		
	–115.685656		
$H_2 + CH_2O \rightarrow CH_3OH$	–0.026832	16.8	–70.5
	–0.013521	–8.5	–35.5

The calculations, which were carried out without any additional solvent models, show that in the first step of the reaction (**A** → **B**) $H_2C{=}O$ forms an adduct to the catalyst by an N–H···O=C hydrogen bond with one of the two pyrazole NH groups and a weak Ru–H···H–C interaction. This adduct formation is exothermic as expected, but slightly endergonic. Then a concerted transfer of the NH proton and the Ru–hydrido ligand takes place via a first transition state (**TS1**). This is quite low in energy and leads to a deprotonated pyrazole unit and a methanol molecule in the coordination sphere of the ruthenium centre bound by an N···H–O–C and a (weak) Ru···H–C interaction (**C**). Compared to the starting material **B**, this hydrogen-transfer step is almost thermoneutral, probably because the coordination number of the ruthenium(II) centre is reduced from six to five. This is supported by the very small barrier for the addition of dihydrogen ($\Delta H^{\ddagger}$ = +0.9 kcal mol^{-1}) in the following reaction (**TS2**) and the pronounced stabilization of the resulting six-coordinate non-classical hydrogen complex **D**. Now a retransfer of the proton to the deprotonated pyrazole site occurs simultaneously with a splitting of the dihydrogen ligand into a ruthenium-bound hydrido ligand and an oxygen-bound proton (**D** → **TS3** → **E**). The reaction is finished by an endothermic elimination of the methanol from the coordination sphere of the catalyst. Details on the calculations can be found in the Supporting Information.

Catalysis

According to the results of the quantum chemical calculations, the barriers for the correlated proton and hydride transfer as well as for the hydrogen uptake by the ruthenium complex should be low. We therefore investigated the hydrogenation and transfer hydrogenation of acetophenone catalyzed by the ruthenium complexes mentioned above. The results are summarized in Table 2.

Table 2. Hydrogenation (h.) and transfer hydrogenation (t.h.) of acetophenone with a series of ruthenium complexes bearing pyrazole-based ligands.

Entry	Catalyst	Hydrogen source[a]	T [°C]	Time [h]	Yield [%][b]
1	**7**	h.	21	2	0
2	**7**	h.	80	2	> 99
3	**7**	t.h.	21	2	0
4	**7**	t.h.	80	2	39
5	**7**	t.h.	80	6	95
6	**8**	h.	21	2	0
7	**8**	h.	80	2	16
8	**8**	h.	80	21	96
9	**9b**	h.	21	2	0
10	**9b**	h.	80	2	18
11	**10b**	h.	21	2	0
12	**10b**	h.	80	2	79
13	**10b**	t.h.	20	2	0
14	**10b**	t.h.	80	2	3
15	**11b**	h.	21	2	0
16	**11b**	h.	80	2	19

[a] Hydrogenation (h.): P_{H2} = 40 bar; transfer hydrogenation (t.h.): with 2-propanol. [b] Yields determined by GC–MS.

Table 2 clearly shows that all the ruthenium complexes investigated show only moderate activity. At room temperature they are almost inactive. Compound **7** (cationic chloridoruthenium complex with a tridentate N,N,N-donor) shows good activity at 80 °C under hydrogenation conditions (Entry 2: P_{H2} = 40 bar) and reduced activity under transfer hydrogenation conditions (Entries 4 and 5: 39 and 95% conversion after 2 and 6 h, respectively). This is in contrast to the behaviour of compound **8**, where the ruthenium centre is coordinated with the same ligand in its twofold deprotonated state. However, here a carbonyl ligand is coordinated to the ruthenium atom, which is probably responsible for a strong decrease in hydrogenation activity (Entries 7 and 8: 16 and 96% conversion after 2 and 21 h, respectively).

Compounds **9b** and **11b** differ slightly in their hydrogenation activity (Entries 10 and 16: 18 and 19% conversion after 2 h), which is not surprising since **11b** should be formed from **9b** in the presence of a base (here: KO*t*Bu). In contrast, compound **10b** (Entry 12: 79% conversion after 2 h) is much more active than compound **9b**. These two complexes differ solely in the nature of the N,N-chelate ligand (pyrazolylpyridine versus bipyrazol). The difference in the hydrogenation activity can be explained by the different electronic influence of either the pyridine or the pyrazole moiety. To elucidate this, in the future we will investigate ligands equipped with electron-donating and -withdrawing groups at the pyrazole ring.[7] On the other hand, the difference

might be explained by the orientation of the hydrido ligand with respect to the acidic pyrazole unit. As already mentioned above, the hydrido ligand in **9a** is located in the *trans* position to the pyrazole ligand, we expect a similar situation for **9b**. In **10b**, which is the best catalyst in our series bearing a carbonyl ligand, the hydrido ligand comes close to the protic N–H unit of a pyrazole moiety, which should be ideal for metal–ligand-bifunctional hydrogenation.

In summary, it has to be mentioned here that the catalytic activities of the (pyrazole)ruthenium complexes are not as high as suggested by the low barriers of activation derived from DFT calculations (see Figure 6). We assign this disagreement to the choice of our model system. We have employed formaldehyde as the substrate, the smallest aldehyde molecule, which additionally possesses a strongly electrophilic carbonyl carbon atom. Furthermore, we have found that switching from triphenylphosphane to trimethylphosphane largely enhances the catalytic activity of related ruthenium complexes in hydrogenation reactions, probably because of steric effects.

Conclusions

Reaction of pyrazole-containing bi- and tridentate chelate ligands with the ruthenium precursors $RuCl_2(PPh_3)_3$, $RuHCl(CO)(PPh_3)_3$ and $RuH_2(CO)(PPh_3)_3$ resulted in the formation of the corresponding chelate complexes. Depending on the nature of the ruthenium precursor, deprotonation of the acidic pyrazole N–H groups can occur. On the other hand ruthenium complexes possessing both an acidic N–H unit and a hydridic Ru–H moiety can be generated. DFT calculations on a model system with a tridentate ligand show relatively low activation barriers for the metal–ligand-bifunctional hydrogenation of formaldehyde. Catalytic studies prove the activity of these complexes in the hydrogenation and transfer hydrogenation of acetophenone. The activity of the complexes investigated can be related to the ligand pattern and be explained with the influence of the other ligands and the electronic and structural situation of the N–H and the Ru–H units.

In the future we will investigate the electronic influence of a series of functionalized pyrazolylpyridines, which can be done without changing steric factors. A further task will be the application of chiral pyrazole-derived ligands for enantioselective hydrogenation reactions.

Experimental Section

5,5′-Dibutyl-1*H*,1′*H*-3,3′-bipyrazole (3b): 5,7,8,10-Tetraoxotetradecane (7.00 g, 27.5 mmol) was dissolved in EtOH (130 mL) and heated to 60 °C. Hydrazine hydrate (3.70 g, 74.0 mmol) was then added slowly, and the mixture was heated under reflux for 4.5 h. The solvent was removed under reduced pressure, and the pale-yellow solid was recrystallized from ethyl acetate. Yield 2.85 g (42%). IR (KBr): $\tilde{\nu}$ = 3180 (s), 3144 (s), 3087 (s), 3034 (s), 2960 (s), 2930 (s), 2872 (s), 2858 (s), 1577 (s), 1464 (m), 1435 (m), 1409 (m), 1379 (w), 1347 (w), 1305 (w), 1270 (m), 1197 (w), 1137 (m), 1061 (w), 1036 (m), 947 (m), 847 (m), 781 (m), 729 (w) cm^{-1}. ^1H NMR (400 MHz, CD_3OD): δ = 6.39 (s, 2 H, H_{Pz}), 2.66 (t, $^3J_{HH}$ = 7.4 Hz, 4 H, H_{Bu}), 1.69–1.62 (m, 4 H, H_{Bu}), 1.39 (m, 4 H, H_{Bu}), 0.95 (t, $^3J_{HH}$ = 7.4 Hz, 6 H, H_{Bu}) ppm. ^{13}C NMR (101 MHz, [D_6]-DMSO): δ = 143.8, 100.10, 30.9, 24.4, 21.6, 13.5 ppm.

[2,6-Bis(5-butyl-1*H*-pyrazol-3-yl)pyridine]chloridobis(triphenylphosphane)ruthenium Chloride (7): Ligand **1** (119 mg, 0.37 mmol) and $(PPh_3)_3RuCl_2$ (355 mg, 0.37 mmol) were dissolved in dry CH_2Cl_2 (10 mL) and stirred at 25 °C for 2 h. The solvent was removed, and the remaining solid was washed twice with diethyl ether (15 mL). Yield 302 mg (80%), orange-coloured solid. IR (KBr): $\tilde{\nu}$ = 3438 (w, N–H), 2927 (m), 2360 (w), 1635 (m), 1558 (m), 1433 (m), 1221 (w), 1093 (m), 748 (m), 699 (s), 517 (s) cm^{-1}. ^1H NMR (600 MHz, CD_3OD): δ = 7.28–7.12 (m, 31 H, H_{Ph}, H_{Py}), 6.97 (d, $^3J_{HH}$ = 7.9 Hz, 2 H, H_{py}), 6.40 (s, 2 H, H_{Pz}), 2.54 (t, $^3J_{HH}$ = 7.3 Hz, 4 H, H_{Bu}), 1.43–1.38 (m, 4 H, H_{Bu}), 1.13–1.07 (m, 4 H, H_{Bu}), 0.83 (t, $^3J_{HH}$ = 7.3 Hz, 6 H, H_{Bu}) ppm. ^{13}C NMR (150.09 MHz, CD_3OD): δ = 154.9, 154.1, 149.6, 134.7–134.6 (m), 132.4 (t, $^1J_{CP}$ = 19.2 Hz), 130.6, 129.0 (t, $^2J_{CP}$ = 4.8 Hz), 119.5, 104.0, 32.5, 26.2, 22.7, 14.1 ppm. ^{31}P NMR (242.9 MHz, CD_3OD): δ = 24.13 (s) ppm. $C_{55}H_{55}Cl_2N_5P_2Ru$ (1019.98): calcd. C 64.76, H 5.44, N 6.86; found C 61.85, H 5.42, N 6.70.

Carbonylbis(triphenylphosphane)[5,5′-pyridine-2,6-diylbis(3-butylpyrazol-1-ido)]ruthenium (8). Method A: $[RuH_2(CO)(PPh_3)_3]$ (50 mg, 72.0 μmol) and ligand **1** (29.4 mg, 90 μmol) were dissolved in dry toluene (10 mL) and heated to reflux for 5 h. The solvent was removed, and the raw product was purified by column chromatography (Al_2O_3/ethyl acetate) to give a yellow solid in 20% yield. **Method B:** Compound **7** (250 mg 0.25 mmol) was dissolved in dry toluene (20 mL). Carbon monoxide was bubbled through the solution, KO*t*Bu (84.1 mg, 0.75 mmol) was added, and the mixture was heated to reflux for 5 h. After the solvent was removed, the raw product was purified by column chromatography (Al_2O_3/ethyl acetate). Yield 160 mg (59%), yellow solid. IR (KBr): $\tilde{\nu}$ = 2928 (m), 1961 (s, C=O), 2954 (s), 1605 (m), 1555 (m), 1480 (m), 1433 (m), 1358 (w), 1321 (w), 1181 (w), 1153 (w), 1093 (m), 1022 (w), 742 (m), 694 (s), 590 (w), 518 (s) cm^{-1}. ^1H NMR (400 MHz, C_6D_6): δ = 7.60–7.55 (m, 12 H, H_{Ph}), 7.2–6.9 (m, 18 H, H_{Ph}), 6.78 (t, $^3J_{HH}$ = 7.7 Hz, 1 H, H_{Py}), 6.24 (d, $^3J_{HH}$ = 7.7 Hz, 2 H, H_{Py}), 6.03 (s, 2 H, H_{Pz}), 2.99 (t, $^3J_{HH}$ = 7.3 Hz, 4 H, H_{Bu}), 1.82–1.75 (m, 4 H, H_{Bu}), 1.47–1.41 (m, 4 H, H_{Bu}), 1.10 (t, $^3J_{HH}$ = 7.3 Hz, 4 H, H_{Bu}) ppm. ^{13}C NMR (150.92 MHz, C_6D_6): δ = 206.3 (t, $^2J_{CP}$ = 15.2 Hz, CO), 155.0, 152.9, 149.8, 136.6, 134.7 (t, $^2J_{CP}$ = 5.5 Hz), 131.1 (t, $^1J_{CP}$ = 22.2 Hz), 129.6, 111.8, 102.1, 33.4, 29.3, 22.9, 14.4 ppm. ^{31}P NMR (161.97 MHz, $CDCl_3$): δ = 32.00 (s) ppm. $C_{56}H_{53}N_5OP_2Ru$ (975.07): calcd. C 68.98, H 5.48, N 7.18; found C 68.29, H 5.40, N 7.24.

General Procedure for the Synthesis of Ruthenium Complexes of the Type [LRuH(CO)(PPh$_3$)$_2$]Cl (9, 10): $[RuHCl(CO)(PPh_3)_3]$ (0.16 mmol) was dissolved in dry THF (15 mL). The corresponding pyrazole (0.16 mmol) was added, and the mixture was heated to reflux for 2 h. After cooling to room temperature the resulting solid was filtered off and washed thoroughly with diethyl ether.

(Carbonyl)(hydrido)[2-(1*H*-pyrazol-3-yl)pyridine]bis(triphenylphosphane)ruthenium Chloride (9a): Yield 81%, colourless solid. IR (KBr): $\tilde{\nu}$ = 3430 (m, NH), 1949 (s, C=O), 1610 (w), 1480 (w), 1433 (m), 1092 (m), 750 (w), 696 (m), 521 (s), 496 (w) cm^{-1}. ^1H NMR (600 MHz, $CDCl_3$): δ = 15.42 (s, 1 H, NH), 7.38 (d, $^3J_{HH}$ = 2.2 Hz, 1 H, H_{Pz}), 7.20–7.06 (m, 32 H, H_{Ph}, H_{Py}), 6.26 (d, $^3J_{HH}$ = 2.1 Hz, 1 H, H_{Pz}), 6.00 (t, $^3J_{HH}$ = 6.4 Hz, 1 H, H_{Py}), –12.50 (t, $^2J_{HP}$ = 19.1 Hz, 1 H, Ru-H) ppm. ^{31}P NMR (242.92 MHz, $CDCl_3$): δ = 46.24 (s) ppm. $C_{45}H_{38}ClN_3OP_2Ru$ (835.27): calcd. C 64.71, H 4.58, N 5.03; found C 63.86, H 4.55, N 4.86.

[2-(5-*tert*-Butyl-1*H*-pyrazol-3-yl)pyridine](carbonyl)(hydrido)bis(triphenylphosphane)ruthenium Chloride (9b): Yield 66%, colourless solid. IR (KBr): $\tilde{\nu}$ = 3421 (m, NH), 1952 (s, C=O), 1740 (w), 1610 (w), 1480 (w), 1433 (m), 1212 (w), 1092 (m), 747 (m), 697 (m), 520 (s), 497 (w) cm^{-1}. ^1H NMR (600 MHz, $CDCl_3$/[D$_6$]DMSO): δ = 13.61 (s, 1 H, NH), 7.14–7.10 (m, 2 H, H_{Py}), 7.05–6.95 (m, 18 H, H_{Ph}), 6.94–6.91 (m, 12 H, H_{Ph}), 6.82 (d, $^3J_{HH}$ = 5.6 Hz, 1 H, H_{Py}), 5.98 (s, 1 H, H_{Pz}), 5.73 (t, $^3J_{HH}$ = 5.6 Hz, 1 H, H_{Py}), 0.96 (s, 9 H, H_{tBu}), –12.66 (t, $^2J_{HP}$ = 20.2 Hz, 1 H, Ru-H) ppm. ^{13}C NMR (150.92 MHz, $CDCl_3$/[D$_6$]DMSO): δ = 203.6–203.3 (m, CO), 156.9, 153.73, 149.6, 147.5, 135.8, 132.8–132.7 (m), 131.6–131.3 (m), 129.3, 127.7–127.6 (m), 123.3, 119.8, 99.0, 30.65, 29.3 ppm. ^{31}P NMR (242.93 MHz, $CDCl_3$/[D$_6$]DMSO): δ = 46.36 (s) ppm. $C_{49}H_{46}ClN_3OP_2Ru$ (891.38): calcd. C 66.02, H 5.20, N 4.71; found C 65.97, H 5.44, N 4.45.

(1*H*,1′*H*-3,3′-Bipyrazole)(carbonyl)(hydrido)bis(triphenylphosphane)ruthenium Chloride (10a): Yield 75%, colourless solid. IR (KBr): $\tilde{\nu}$ = 3429 (m, NH), 3053 (w), 2853 (w), 2825 (w), 1941 (s, C=O), 1622 (w), 1480 (w), 1433 (m), 1093 (m), 749 (w), 695 (m), 521 (m), 495 (w) cm^{-1}. ^1H NMR (400 MHz, [D$_6$]DMSO): δ = 14.13 (s, 1 H, NH′), 12.82 (s, 1 H, NH), 7.77 (s, 1 H, H_{Pz}′), 7.49–7.25 (m, 31 H, H_{Ph}, H_{Pz}), 6.47 (s, 1 H, H_{Pz}′), 6.33 (s, 1 H, H_{Pz}), –12.19 (t, $^2J_{H-P}$ = 20.3 Hz, 1 H, Ru-H) ppm. ^{13}C NMR (150.9, [D$_6$]DMSO): δ = 204.2–203.9 (m, CO), 144.3, 143.9, 133.1 (t, J_{PC} = 5.7 Hz), 132.8–132.5 (m), 129.9, 128.3, 102.3, 102 ppm. ^{31}P NMR (161.9 MHz, $CDCl_3$): δ = 44.97 (s) ppm. $C_{43}H_{37}ClN_4OP_2Ru$ (824.25): calcd. C 62.66, H 4.52, N 6.80; found C 62.08, H 4.70, N 7.31.

(5,5′-Dibutyl-1*H*,1′*H*-3,3′-bipyrazole)(carbonyl)(hydrido)bis(triphenylphosphane)ruthenium Chloride (10b): Yield 68%, colourless solid. IR (KBr): $\tilde{\nu}$ = 3429 (m, NH), 2927 (m), 1948 (s), 1625 (w), 1570 (w), 1497 (w), 1433 (m), 1092 (m), 808 (w), 743 (w), 695 (s), 595 (w), 518 (s), 497 (w) cm^{-1}. ^1H NMR (400 MHz, [D$_6$]DMSO): δ = 13.60 (s, 1 H, NH′), 12.27 (s, 1 H, NH), 7.43–7.42 (m, 30 H, H_{Ph}), 6.20 (s, 1 H, H_{Pz}′), 6.07 (s, 1 H, H_{Pz}), 2.03 (t, $^3J_{HH}$ = 7.5, 4 H, H_{Bu}), 1.48–1.40 (m, 4 H, H_{Bu}), 1.27–1.04 (m, 8 H, H_{Bu}), 0.87–0.82 (m, 6 H, H_{Bu}), –12.10 (t, $^2J_{H-P}$ = 20.4, 1 H, H-Ru) ppm. ^{13}C NMR (150.91 MHz, MeOD): δ = 205.6–205.3 (m, CO), 150.4, 149.6, 146.4, 134.8–134.7 (m), 134.6, 134.5, 131.0, 129.2 (t, $^2J_{PC}$ = 4.6 Hz), 101.9, 101.6, 32.6, 31.87, 26.3, 23.0, 14.1, 14.0 ppm. ^{31}P NMR (242.94 MHz, MeOD): δ = 43.91 (s) ppm. $C_{51}H_{53}ClN_4OP_2Ru$ (936.46): calcd. C 65.41, H 5.71, N 5.98; found C 65.55, H 5.84, N 5.52.

(Carbonyl)(hydrido)[5-(pyridin-2-yl)pyrazol-1-ido]bis(triphenylphosphane)ruthenium (11a): [$RuH_2(CO)(PPh_3)_3$] (140 mg, 0.15 mmol) and 2-(1*H*-pyrazol-3-yl)pyridine (22 mg, 0.15 mmol) were dissolved in dry toluene (10 mL) and stirred under reflux for 2 h. The resulting colourless solid was filtered off and washed thoroughly with toluene and diethyl ether. Yield 101 mg (87%). IR (KBr): $\tilde{\nu}$ = 3051 (w), 1923 (s, CO), 1602 (w), 1529 (w), 1480 (w), 1447 (m), 1434 (m), 1094 (w), 742 (w), 695 (m), 517 (m) cm^{-1}. ^1H NMR (400 MHz, $CDCl_3$): δ = 7.94 (d, $^3J_{HH}$ = 5.3 Hz, 1 H, H_{Py}), 7.45–7.41 (m, 2 H, H_{Py}, H_{Pz}), 7.36–7.30 (m, 12 H, H_{Ph}), 7.23–7.13 (m, 18 H, H_{Ph}), 6.89 (d, $^3J_{HH}$ = 7.9 Hz, 1 H, H_{Py}), 6.40 (t, $^3J_{HH}$ = 5.9 Hz, 1 H, H_{Py}), 6.15 (d, $^3J_{HH}$ = 1.5 Hz, 1 H, H_{Pz}), –10.37 (t, $^2J_{HP}$ = 20.2 Hz, 1 H, RuH) ppm. ^{31}P NMR (161.9 MHz, $CDCl_3$): δ = 45.66 (s) ppm. $C_{45}H_{37}N_3OP_2Ru$ (798.82): calcd. C 67.66, H 4.67, N 5.26; found C 66.74, H 4.56, N 5.10. The solubility of this compound is too low to record a ^{13}C NMR spectrum.

[3-*tert*-Butyl-5-(pyridin-2-yl)pyrazol-1-ido](carbonyl)(hydrido)bis(triphenylphosphane)ruthenium (11b): [$RuH_2(CO)(PPh_3)_3$] (50 mg, 72.0 μmol) and 2-(5-*tert*-butyl-1*H*-pyrazol-3-yl)pyridine (18.2 mg, 90 μmol were dissolved in dry toluene (10 mL) and heated to reflux for 72 h. After cooling to room temperature, pentane (10 mL) was added. The precipitated colourless solid was filtered off and washed

Table 3. Summary of the crystallographic data and details of data collection and refinement for compounds **3b**, **7**, **8**, **9a** and **10b**.

	3b	**7**	**8**	**9a**	**10b**
Empirical formula	$C_{14}H_{22}N_4$	$C_{55}H_{55}Cl_2N_5P_2Ru$	$C_{56}H_{53}N_5OP_2Ru$	$C_{46}H_{39}Cl_4N_3OP_2Ru$	$C_{53}H_{59}ClN_4O_2P_2Ru$
M_r [g mol^{-1}]	246.36	1019.95	975.04	954.61	982.50
Crystal size [mm]	0.40 × 0.28 × 0.10	0.14 × 0.11 × 0.08	0.12 × 0.06 × 0.04	0.14 × 0.07 × 0.04	0.28 × 0.26 × 0.12
T [K]	150(2)	150(2)	150(2)	150(2)	293(2)
λ [Å]	1.54184	0.71073	1.54184	1.54184	0.71073
Crystal system	tetragonal	monoclinic	monoclinic	triclinic	monoclinic
Space group	$I4_1/a$	$P2_1/c$	$P2_1/n$	$P\bar{1}$	Cc
a [Å]	12.5762(2)	12.3066(2)	14.4507(2)	9.295(3)	24.6004(16)
b [Å]	12.5762(2)	16.6012(3)	21.4693(3)	19.736(8)	9.8153(5)
c [Å]	18.2475(5)	25.5794(4)	15.4743(2)	25.897(8)	23.5948(14)
α [°]	90	90	90	68.40(3)	90
β [°]	90	91.136(2)	98.5410(10)	88.11(2)	117.497(7)
γ [°]	90	90	90	81.37(3)	90
V [Å^3]	2886.04(10)	5224.96(15)	4747.60(11)	4366(3)	5053.6(5)
Z	8	4	4	4	4
$\rho_{calcd.}$ [g cm^{-3}]	1.134	1.297	1.364	1.452	1.291
μ [mm^{-1}]	0.545	0.504	3.665	6.158	0.469
θ range [°]	6.95–62.66	2.45–32.48	3.91–62.64	3.67–62.50	2.30–28.17
Measured reflections	3324	71068	23051	34979	30310
Independent reflections	1137 [R_{int} = 0.0267]	17334 [R_{int} = 0.1069]	7487 [R_{int} = 0.0275]	13540 [R_{int} = 0.0344]	12257 [R_{int} = 0.0405]
Data/restraints/param.	1137/0/83	17334/0/586	7487/0/586	13540/0/1033	12257/2/576
Final R indices $[I > 2\sigma(I)]$[a]	0.0435, 0.1252	0.0631, 0.1250	0.0247, 0.0533	0.0264, 0.0638	0.0322, 0.0592
R indices (all data)[b]	0.0495, 0.1276	0.1443, 0.1522	0.0374, 0.0567	0.0393, 0.0782	0.0535, 0.0630
GoF[c]	1.123	0.964	0.925	1.051	0.843
Flack parameter	–	–	–	–	0.271(18)
$\Delta\rho_{max}/\rho_{min}$ [e Å^{-3}]	0.175/–0.186	0.961/–0.616	0.222/–0.425	0.619/–0.605	0.414/–0.441

[a] $R_1 = \Sigma||F_o| - |F_c||/\Sigma|F_o|$. [b] $wR_2 = \{\Sigma[w(F_o^2 - F_c^2)^2]/\Sigma[w(F_o^2)^2]\}^{1/2}$. [c] GoF = $\{\Sigma[w(F_o^2 - F_c^2)^2]/(n - p)\}^{1/2}$.

thoroughly with pentane. Yield 44.5 mg (70%). IR (KBr): $\tilde{\nu}$ = 3054 (w), 2957 (w), 1917 (s, CO), 1604 (w), 1481 (w), 1434 (m), 1260 (w), 1093 (m), 804 (w), 744 (w), 695 (m), 517 (s) cm^{-1}. ^1H NMR (600 MHz, [D$_6$]DMSO): δ = 7.84 (br. s, 1 H), 7.4–7.1 (m, 31 H), 6.89 (br. s, 1 H), 6.47 (br. s, 1 H), 5.95 (br. s, 1 H), 1.04 (br. s, 9 H), –10.49 (br. s, 1 H, RuH) ppm. ^{31}P NMR (242.94 MHz, [D$_6$]-DMSO): δ = 46.49 (s) ppm. $C_{49}H_{45}N_3OP_2Ru$ (854.93): calcd. C 68.84, H 5.30, N 4.91; found C 69.32, H 5.41, N 4.83. The solubility of this compound is too low to record a ^{13}C NMR spectrum.

Catalyses: The hydrogenation reactions were carried out in a laboratory autoclave (Berghof HR-200) with a hydrogen pressure of 40 bar. The catalyst (0.02 mmol) and KO*t*Bu (5 mmol) were suspended in 2-propanol (20 mL) in a Schlenk tube under inert conditions. The autoclave was filled with nitrogen, the mixture mentioned above and acetophenone (10 mL). After closing, the autoclave was purged three times with hydrogen up to a pressure of 8 bar and finally pressurized up to 40 bar. The transfer hydrogenations were carried out in a Schlenk tube: a mixture of 2-propanol (20 mL), the catalyst (0.02 mmol) and KO*t*Bu (5 mmol) were heated to 80 °C. The acetophenone was added at this temperature. The yields were determined by GC–MS with dodecane as the internal standard.

X-ray Structure Analyses: Crystal data and refinement parameters are collected in Table 3. The structures were solved by direct methods (for compounds **3b**, **7**, **8** and **9a** SIR92[26] and for compound **10b** SIR97[27]), completed by subsequent difference Fourier syntheses and refined by full-matrix least-squares procedures.[28] Semiempirical absorption corrections from equivalents (Multiscan) were carried out for **3b**, **8** and **9a**. For compound **7** no absorption correction was performed, whereas for compound **10b** an analytical absorption correction was used. All non-hydrogen atoms were refined with anisotropic displacement parameters. All hydrogen-atom positions were calculated in ideal positions (riding model) except for the hydrogen atoms bound to ruthenium atoms in compounds **9a** and **10b**, which were located in the difference Fourier synthesis and were then refined semifreely while constraining their *U* values to 1.2 times the *U*(eq) values of the corresponding Ru atoms. Because of the presence of severely disordered solvent molecules, the SQUEEZE process implemented in PLATON was performed for compound **7**. Detailed information on this has been posted in the corresponding CIF file. CCDC-786064 (**3b**), -786065 (**7**), -786066 (**8**), -786063 (**9a**) and -786067 (**10b**) contain the supplementary crystallographic data for this paper. These data can be obtained free of charge from The Cambridge Crystallographic Data Centre via www.ccdc.cam.ac.uk/data_request/cif.

Quantum Chemical Calculations: These were performed with the program Gaussian 03[29] by using the B3LYP gradient-corrected exchange-correlation functional[13] in combination with the 6-311+G** basis set.[14] Full geometry optimizations were carried out in C_1 symmetry by using analytical gradient techniques, and the resulting structures were confirmed to be true minima by diagonalization of the analytical Hessian Matrix.

Supporting Information (see footnote on the first page of this article): Spectroscopic data, X-ray data, data of the theoretical calculations.

[1] a) R. Noyori, T. Ohkuma, *Angew. Chem.* **2001**, *113*, 40–75; *Angew. Chem. Int. Ed.* **2001**, *40*, 40–73; b) R. Noyori, *Angew. Chem.* **2002**, *114*, 2108–2123; *Angew. Chem. Int. Ed.* **2002**, *41*, 2008–2022.

[2] a) R. Noyori, M. Yamakawa, S. Hashiguchi, *J. Org. Chem.* **2001**, *66*, 7931–7944; b) K. Muniz, *Angew. Chem.* **2005**, *117*, 6780–6785; *Angew. Chem. Int. Ed.* **2005**, *44*, 6622–6627; c) S. E. Clapham, A. Hadzovic, R. H. Morris, *Coord. Chem. Rev.* **2004**, *248*, 2201–2237; d) M. Yamakawa, H. Ito, R. Noyori, *J. Am. Chem. Soc.* **2000**, *122*, 1466–1478; e) C. A. Sandoval, T. Ohkuma, K. Muniz, R. Noyori, *J. Am. Chem. Soc.* **2003**, *125*, 13490–13503; f) M. Lei, W. C. Zhang, Y. Chen, Y. H. Tang, *Organometallics* **2010**, *29*, 543–548.

[3] S. Bergner, G. Wolmershäuser, H. Kelm, W. R. Thiel, *Inorg. Chim. Acta* **2008**, *361*, 2059–2069.

[4] a) Y. Kashiwame, S. Kuwata, T. Ikariya, *Chem. Eur. J.* **2010**, *16*, 766–770; b) A. Mukherjee, A. Sarkar, *Arkivoc* **2003**, 87–95; c) H. Willms, W. Frank, C. Ganter, *Organometallics* **2009**, *28*, 3049–3058; d) W. R. Thiel, T. Priermeier, *Angew. Chem.* **1995**, *107*, 1870–1872; *Angew. Chem. Int. Ed. Engl.* **1995**, *34*, 1737–1738; e) A. Hroch, G. Gemmecker, W. R. Thiel, *Eur. J. Inorg. Chem.* **2000**, *3*, 1107–1114; f) H. Glas, M. Barz, W. R. Thiel, *J. Organomet. Chem.* **2001**, *621*, 153–157.

[5] a) J. G. Malecki, J. O. Dziećgielewski, R. Kruszynski, T. J. Bartczak, *Inorg. Chem. Commun.* **2003**, *6*, 721–724; b) E. W. Evans, M. T. Atlay, *Synth. React. Inorg. Met.-Org. Chem.* **2001**, *31*, 623–632; c) H. Adams, W. Z. Alsindi, M. Davies, M. B. Duriska, T. L. Easun, H. E. Fenton, J. M. Herrera, M. W. George, K. L. Ronayne, X. Z. Sun, M. Towrie, M. D. Ward, *Dalton Trans.* **2006**, 39–50; d) S. Huh, Y. Kim, K. T. Youm, M. J. Jun, *Polyhedron* **1999**, *18*, 2625–2631; e) D. Carmona, J. Ferrer, I. M. Marzal, L. A. Oro, *Gazz. Chim. Ital.* **1994**, *124*, 35–42.

[6] a) D. Zabel, A. Schubert, G. Wolmershäuser, R. L. Jones Jr., W. R. Thiel, *Eur. J. Inorg. Chem.* **2008**, 3648–3654; b) A.-K. Pleier, H. Glas, M. Grosche, P. Sirsch, W. R. Thiel, *Synthesis* **2001**, 55–62.

[7] W. R. Thiel, J. Eppinger, *Chem. Eur. J.* **1997**, *3*, 696–705.

[8] F. Effenberger, *Chem. Ber.* **1965**, *98*, 2260–2265.

[9] a) S. Bondock, W. Fadaly, M. A. Metwally, *Eur. J. Med. Chem.* **2009**, *44*, 2813–4818; b) T. Jozak, M. Fischer, J. Thiel, Y. Sun, H. Kelm, W. R. Thiel, *Eur. J. Org. Chem.* **2009**, 1445–1452; c) A. V. Velikorodov, V. B. Kovalev, O. O. Krivosheev, *Russ. J. Org. Chem.* **2009**, *45*, 1208–1209; d) D. Sanz, R. M. Claramunt, I. Alkorta, J. Elguero, W. R. Thiel, T. Rüffer, *New J. Chem.* **2008**, *32*, 2225–2232.

[10] See the following publications and literature cited therein: a) R. M. Claramunt, P. Cornago, V. Torres, E. Pinilla, M. R. Torres, A. Samat, V. Lokshin, M. Valés, J. Elguero, *J. Org. Chem.* **2006**, *71*, 6881–6891; b) R. M. Claramunt, P. Cornago, M. D. Santa María, V. Torres, E. Pinilla, M. R. Torres, J. Elguero, *Supramol. Chem.* **2006**, *18*, 349–356; c) A. Levai, A. M. S. Silva, J. A. S. Cavaleiro, I. Alkorta, J. Elguero, J. Jeko, *Eur. J. Org. Chem.* **2006**, 2825–2832.

[11] T. A. Stephenson, G. Wilkinson, *J. Inorg. Nucl. Chem.* **1966**, 945–956.

[12] N. Ahmad, J. J. Levison, S. D. Robinson, M. F. Uttlky, E. R. Wonchobs, G. W. Parshall, *Inorg. Synth.* **1974**, *15*, 45–64.

[13] a) S. Sharma, M. Chandra, D. S. Pandey, *Eur. J. Inorg. Chem.* **2004**, 3555–3563; b) K. S. Singh, Y. A. Mozharivskyj, M. R. Kollipara, *Z. Anorg. Allg. Chem.* **2006**, *632*, 172–179; c) S. B. Billings, M. T. Mock, K. Wiacek, M. B. Turner, W. S. Kassel, K. J. Takeuchi, A. L. Rheingold, W. J. Boyko, C. A. Bessel, *Inorg. Chim. Acta* **2003**, *355*, 103–115; d) D. Mishra, S. Naskar, S. K. Chattopadhyay, M. Maji, P. Sengupta, R. Dinda, S. Ghosh, T. C. W. Mak, *Trans.-Met. Chem.* **2005**, *30*, 352–356; e) C. A. Bessel, R. F. See, D. L. Jameson, M. R. Churchill, K. J. Takeuchi, *J. Chem. Soc., Dalton Trans.* **1991**, 2801–2805; f) S. Sharma, S. K. Singh, M. Chandra, D. S. Pandey, *J. Inorg. Biochem.* **2005**, *99*, 458–466.

[14] S. Naskar, M. Bhattacharjee, *J. Organomet. Chem.* **2005**, *690*, 5006–5010.

[15] a) I. Serrano, M. Rodriguez, I. Romero, A. Llobet, T. Parella, J. M. Campelo, D. Luna, J. M. Marinas, J. Benet-Buchholz, *Inorg. Chem.* **2006**, *45*, 2644–2651; b) J. Mola, M. Rodriguez, I. Romero, A. Llobet, T. Parella, A. Poater, M. Duran, M. Sola, J. Benet-Buchholz, *Inorg. Chem.* **2006**, *45*, 10520–10529.

[16] L. Dahlenburg, H. Treffert, J. Dannhauser, F. W. Heinemann, *Inorg. Chim. Acta* **2007**, *360*, 1474–1481.
[17] a) N.-Y. Sun, S. J. Simpson, *J. Organomet. Chem.* **1992**, *434*, 341–349; b) M. D. Hargreaves, M. F. Mahon, M. K. Whittlesey, *Inorg. Chem.* **2002**, *41*, 3137–3145.
[18] J. W. Slater, D. M. D′Alessandro, F. R. Keene, P. J. Steel, *Dalton Trans.* **2006**, 1954–1962.
[19] L. A. Watson, O. V. Ozerov, M. Pink, K. G. Caulton, *J. Am. Chem. Soc.* **2003**, *125*, 8426–8427.
[20] a) D. Carmona, J. Ferrer, L. A. Oro, M. C. Apreda, C. Foces-Foces, F. H. Cano, J. Elguero, M. L. Jimeno, *J. Chem. Soc., Dalton Trans.* **1990**, 1463–1475; b) M. M. Taqui Khan, P. S. Roy, K. Venkatasubramanian, N. H. Khan, *Inorg. Chim. Acta* **1990**, *176*, 49–55.
[21] A. Santos, J. López, A. Galán, J. J. González, P. Tinoco, A. M. Echavarrn, *Organometallics* **1997**, *16*, 3482–3488.
[22] a) A. Romero, A. Vegas, A. Santos, *J. Organomet. Chem.* **1987**, *319*, 103–111; b) S. Gopinathan, S. S. Deshpande, C. Gopinathan, *Z. Anorg. Allg. Chem.* **1985**, *527*, 203–207.
[23] a) C. Lee, W. Yang, R. G. Parr, *Phys. Rev. B* **1988**, *37*, 785–789; b) A. D. Becke, *Phys. Rev.* **1988**, *A38*, 3098–3100; c) B. Miehlich, A. Savin, H. Stoll, H. Preuss, *Chem. Phys. Lett.* **1989**, *157*, 200–206.
[24] a) P. C. Hariharan, J. A. Pople, *Theor. Chim. Acta* **1973**, *28*, 213–222; b) M. M. Francl, W. J. Petro, W. J. Hehre, J. S. Binkley, M. S. Gordon, D. J. DeFrees, J. A. Pople, *J. Chem. Phys.* **1982**, *77*, 3654–3665.
[25] P. J. Hay, W. R. Wadt, *J. Chem. Phys.* **1985**, *82*, 270–283.
[26] A. Altomare, G. Cascarano, C. Giacovazzo, A. Guagliardi, M. C. Burla, G. Polidori, M. Camalli, *J. Appl. Crystallogr.* **1994**, *27*, 435.
[27] A. Altomare, M. C. Burla, M. Camalli, G. L. Cascarano, C. Giacovazzo, A. Guagliardi, A. G. G. Moliterni, G. Polidori, R. Spagna, *J. Appl. Crystallogr.* **1999**, *32*, 115.
[28] G. M. Sheldrick, *SHELX-97: Programs for Crystal Structure Analysis*, University of Göttingen, Göttingen, Germany, **1998**.
[29] M. J. Frisch, G. W. Trucks, H. B. Schlegel, G. E. Scuseria, M. A. Robb, J. R. Cheeseman, J. A. Montgomery Jr., T. Vreven, K. N. Kudin, J. C. Burant, J. M. Millam, S. S. Iyengar, J. Tomasi, V. Barone, B. Mennucci, M. Cossi, G. Scalmani, N. Rega, G. A. Petersson, H. Nakatsuji, M. Hada, M. Ehara, K. Toyota, R. Fukuda, J. Hasegawa, M. Ishida, T. Nakajima, Y. Honda, O. Kitao, H. Nakai, M. Klene, X. Li, J. E. Knox, H. P. Hratchian, J. B. Cross, V. Bakken, C. Adamo, J. Jaramillo, R. Gomperts, R. E. Stratmann, O. Yazyev, A. J. Austin, R. Cammi, C. Pomelli, J. W. Ochterski, P. Y. Ayala, K. Morokuma, G. A. Voth, P. Salvador, J. J. Dannenberg, V. G. Zakrzewski, S. Dapprich, A. D. Daniels, M. C. Strain, O. Farkas, D. K. Malick, A. D. Rabuck, K. Raghavachari, J. B. Foresman, J. V. Ortiz, Q. Cui, A. G. Baboul, S. Clifford, J. Cioslowski, B. B. Stefanov, G. Liu, A. Liashenko, P. Piskorz, I. Komaromi, R. L. Martin, D. J. Fox, T. Keith, M. A. Al-Laham, C. Y. Peng, A. Nanayakkara, M. Challacombe, P. M. W. Gill, B. Johnson, W. Chen, M. W. Wong, C. Gonzalez, J. A. Pople, *Gaussian 03, Revision E.01*, Gaussian, Inc., Wallingford, CT, **2004**.

Received: July 26, 2010
Published Online: September 29, 2010

